Protein Phosphatase 6 Regulatory Subunits Composed of Ankyrin Repeat Domains[†]

Bjarki Stefansson, Takashi Ohama, Abbi E. Daugherty, and David L. Brautigan*

Center for Cell Signaling and Department of Microbiology, University of Virginia School of Medicine, Charlottesville, Virginia 22908

Received November 17, 2007

ABSTRACT: Protein phosphatase 6 (PP6) is an essential Ser/Thr phosphatase conserved among eukaryotes. The *Saccharomyces cerevisiae* homologue of PP6 called Sit4 depends on association with SAPS domain subunits. This study used a human SAPS domain subunit FLAG-PP6R1 to identify endogenous interacting proteins. Mass spectrometry identified coprecipitating proteins as PP6 catalytic subunit and three ankyrin repeat proteins (Ankrd28, Ankrd44, and Ankrd52). These proteins have extensive sequence identity to one another but segregate into separate branches on a phylogenetic tree for vertebrate species, suggesting individual biological functions. Tagged Ankrd28 coprecipitated with PP6, not with PP2A or PP4, and with SAPS domain subunits PP6R1 and PP6R3. Tagged PP6 coprecipitated endogenous SAPS domain subunits and Ankrd28. The C-terminal region of PP6R1 was sufficient to coprecipitate Ankrd28, but not PP6, demonstrating that PP6R1 acts as a scaffold with separate regions for binding to PP6 and to Ankrd28. Endogenous PP6 holoenzymes with PP6R1 and PP6R3 subunits were resolved by DEAE chromatography and eluted together with Ankrd28 at M_r > 440 kDa from Superose 12. Knockdown of PP6R1 or Ankrd28, but not PP6R3, produced equivalent enhancement of IκBϵ degradation in response to TNFα. The results suggest that PP6 functions as a heterotrimer, composed of the PP6 catalytic subunit bound to a SAPS domain scaffold subunit that associates with Ankrd28. We propose that the SAPS and ankyrin repeat regulatory subunits determine the function and specificity of PP6.

Protein phosphatase 6 (PP6) is an essential eukaryotic Ser/Thr phosphatase conserved from yeast to humans. The *Saccharomyces cerevisiae* homologue of PP6, Sit4,[1] is an essential gene, and different temperature sensitive mutations show that Sit4 is required for G_1 to S progression and several other cellular processes (*1*−*15*; for reviews, see refs *16* and *17*). The *Sit4*^{ts} mutant is rescued from G1 arrest by expression of *Schizosaccharomyces pombe* ppe1, *Drosophila* PPV, or human PP6, showing that these are functional homologues of Sit4 (*18*, *19*). The *Sit4*^{ts} phenotype is not reversed by expression of other Ser/Thr phosphatases (PP1 or PP4), indicating that different phosphatases have specific and nonredundant functions. Sit4 associates with three subunits called Sit4-associated proteins SAP155, SAP185, and SAP190 (*2*, *20*). Deletion of all SAP proteins produced a phenotype identical to that caused by deletion of Sit4 itself, demonstrating that SAP and Sit4 proteins depend on one another. Overexpression or deletion of individual SAP proteins produced distinctive phenotypes that demonstrate specific functions for each of these proteins. SAP proteins are therefore thought to be regulatory subunits for Sit4, determining substrate specificity and functions of different Sit4 phosphatase holoenzymes.

The yeast SAP proteins contain a common domain of nearly identical sequence called the SAPS domain. We found that the SAPS domain is conserved among eukaryotes and identified human homologues of the SAP subunits, called PP6R1, PP6R2, and PP6R3 (*21*). These regulatory subunits associate with PP6 but not with PP2A or PP4, the two phosphatases most closely related to PP6. This demonstrates that the SAPS domain discriminates between phosphatases and is specific for PP6. PP6R1 or PP6R2 coprecipitated IκBϵ when each protein was overexpressed. Knockdown of PP6R1 by siRNA increased the level of degradation of IκBϵ in response to TNFα stimulation, consistent with a role for PP6 in limiting NF-κB signaling. Knockdown of PP6R3 did not enhance degradation of IκBϵ, demonstrating that different SAPS domain subunits for PP6 had specific effects.

The goal of this study was to identify proteins that associate with PP6R1, with the expectation that we might identify substrates in complexes with the PP6 holoenzyme. We made a stable cell line expressing FLAG-PP6R1, prepared protein complexes by immunoprecipitation, and identified proteins by mass spectrometry. Besides PP6, we found three related ankyrin repeat proteins. We demonstrate that one ankyrin repeat subunit (ARS-A, Ankrd28) associates with PP6 and all three SAPS-related subunits, on the basis of reciprocal immunoprecipitation of overexpressed proteins. Knockdown of ARS-A enhanced the degradation of IκBϵ after TNFα stimulation, effects comparable to those of

[†] This work supported in part by U.S. Public Health Service Grant CA-77584 (to D.L.B.).

* To whom correspondence should be addressed: Center for Cell Signaling, University of Virginia School of Medicine, P.O. Box 800577, West Complex, MSB 7225, Charlottesville, VA 22908. Telephone: (434) 924-5892. Fax: (434) 243-2829. E-mail: db8g@virginia.edu.

[1] Abbreviations: Ankrd, ankyrin repeat domain; TNF, tumor necrosis factor; CaMKII, calcium/calmodulin-dependent kinase II-δ; GSK3, glycogen synthase kinase-3; NFκB, nuclear factor-κB; ARS, protein phosphatase 6 ankyrin repeat subunit; SAP, Sit4-associated protein; IκBϵ, inhibitor κB-ϵ; Sit4, suppressor of initiation of transcription 4; HA, hemagglutinin (epitope tag with a YPYDVPDYA sequence); PITK, phosphatase interactor targeting K protein.

10.1021/bi7022877 CCC: $40.75
Published on Web 01/11/2008

knockdown of PP6R1. The equivalent effects support our proposal that PP6 exists as heterotrimers composed of a catalytic subunit, an ankyrin repeat subunit, and a SAPS domain subunit.

MATERIALS AND METHODS

Antibodies and Chemicals. Chemicals not otherwise specified were purchased from Fisher Scientific (Hampton, NH). Anti-FLAG and anti-actin antibodies were purchased from Sigma-Aldrich and used at a dilution of 1:1000. Anti-PP1 (sc-7482) and anti-IκBϵ (sc-7156) antibodies were purchased from Santa Cruz Biotechnology and used at a dilution of 1:1000. Anti-GAPDH (MAB374), anti-RCC1 (07−519), and anti-V5 antibodies (AB3792) were purchased from Millipore (Billerica, MA) and used at a dilution of 1:2000. Anti-PP4 (B50318-51) antibodies were purchased from Stratagene and used at a dilution of 1:500. Chicken anti-HA antibodies were purchased from Aves Labs, Inc., and used at a dilution of 1:1000. Goat anti-rabbit Alexa Fluor 680, donkey sheep Alexa Fluor 680, and goat anti-mouse Alexa Fluor 680 antibodies were purchased from Molecular Probes, Invitrogen Technologies, and used at a dilution of 1:3000. Rabbit sheep 800, goat anti-mouse 800, goat anti-rabbit IRDye 800, goat anti-chicken IRDye 680, and goat anti-chicken IRDye 800 antibodies were purchased from Rockland Immunochemicals and used at a dilution of 1:3000. Antibodies against PP2A, PP6, PP6R1, PP6R3, and alpha4 were previously described (*21*, *22*). Antibodies against ARS-A were prepared against a peptide corresponding to residues ^{62}FKKEDVNFQDNEKRTPLHAAAYLGD^{86} in the N-terminus of human ARS-A (GenBank accession number O15084). Antibodies against ARS-A (generous gift from T. A. Haystead, Duke University Medical Center, Durham, NC) corresponding to residues in the C-terminus of human ARS-A were previously described (*23*). TNFα was purchased from R&D Systems, Inc. (Minneapolis, MN). Protease Inhibitor Cocktail Set V (catalog no. 539137) was purchased from Calbiochem. Microcystin-LR was purchased from ALEXIS Biochemicals (San Diego, CA).

Generation of Stable Cell Lines and Mass Spectrometry. Stable HEK293 cell lines were created as described previously (*26*), and immunoprecipitation of FLAG-PP6R1 for mass spectrometry was performed as described, with exceptions. The lysis buffer contained 0.1% Tween 20 instead of 0.5% NP-40. Cells in lysis buffer were passed through a 28G-[1/2] syringe and left on ice for 15 min. After centrifugation at 70 000 rpm for 10 min, the supernatant was incubated with mouse IgG agarose beads (A0919 Sigma) for 1.5 h at 4 °C. Beads were removed, and the supernatant was incubated with anti-FLAG beads for 2 h at 4 °C. After two washes with lysis buffer, the immunoprecipitate was washed twice with buffer containing 50 mM Tris (pH 7.4) and 0.1 M NaCl. FLAG-PP6R1 was eluted by incubating beads for 30 min at room temperature with 1.5 mg/mL FLAG peptide (Sigma) in 25 mM Tris-HCl (pH 7.4). The eluate was reduced with DTT and alkylated with iodoacetamide before addition of 0.5 μg of Promega modified trypsin overnight. A second 0.5 μg of trypsin was added, and digestion was continued for 24 h. The sample was acidified to 5% with acetic acid. The LC−MS system is a Finnigan LTQ-FT mass spectrometer system with a Protana nanospray ion source interfaced to a self-packed 8 cm × 75 μm ID Phenomenex Jupiter 10 um C18 reversed-phase capillary column. Peptides were eluted from the column with an acetonitrile/0.1 M acetic acid gradient at a flow rate of 0.25 μL/min. The nanospray ion source was operated at 2.8 kV, and peptides were analyzed using full scan mass spectra to determine peptide molecular weights and product ion spectra to determine amino acid sequences in sequential scans. The data were analyzed by database searching using the Sequest search algorithm against human IPI.

Sequence Alignment and Construction of the Phylogenetic Tree. Sequence alignment of ARS-A (accession number IPI00477505; aliases, KIAA0379, Ankrd28, PITK), ARS-B (accession number IPI00167419; aliases, Ankrd44, MGC21968, MGC70444), and ARS-C (accession number IPI00398957; aliases, Ankrd52, FLJ34236) was performed using the ClustalW method (default settings at http://www.ebi.ac.uk/clustalw/#). Output for aligned sequences was made using ESPript (http://espript.ibcp.fr/ESPript/ESPript) (*24*). For the phylogenetic tree, ClustalW alignment of ARS-related proteins was carried out using ClustalX 1.83, and ungapped versions of the alignments were created in MacClade 4.05 (http://macclade.org/macclade.html) following a 50% majority rule for deletion of alignment columns with gaps (i.e., columns with >50% of the sequences displaying gaps were removed from the alignment). The Parsimony Consensus (unrooted) tree was generated using the ProtPars program in Phylip 3.66 [Felsenstein, J. (2005) *PHYLIP (Phylogeny Inference Package)*, version 3.6, distributed by the author at the Department of Genome Sciences, University of Washington, Seattle] using the degapped Clustal alignment. Multiple protpars runs, using multiple random input orders, yielded a total of 60 equally parsimonious trees (length of 5559 steps). The figure shows the majority rule consensus of these trees, rooted with the insect sequences. Branch lengths for the phylogram of the parsimony consensus tree were calculated under protein maximum likelihood using the Proml program in Phylip 3.66. The bootstrap proportions are from 10 000 replications, using ProtPars and random input order for each replication.

Plasmids. DNA for human PP6R3 was amplified by PCR from HeLa cDNA generated by Thermoscript poly(dT) reverse transcription PCR (Invitrogen) following the manufacturer's protocol. The primers for PCR of PP6R3 were 5′-GAA TTC ATG TTT TGG AAA TTT GAT CTT CAC T-3′ (forward primer) and 5′-CTC GAG TAC AGG GCC ATT CAC TGA AGT-3′ (backward primer). PP6R3 PCR inserts, which matched the open reading frame of BC105934.1, were ligated in-frame with the FLAG epitope at the EcoRI and XhoI sites in mammalian expression vector pcDNA3-FLAG. PP6R1 PCR insert (encoding the protein sequence depicted for accession number AAI11981.1) was ligated in-frame with the FLAG epitope at the EcoRI and XhoI sites in mammalian expression vector pcDNA3-FLAG. DNA for human ARS-A was amplified by PCR from a cDNA clone (Clone ID hh00505s1) generously provided by Kazusa DNA Research Institute (Kisarazu, Chiba, Japan). The primers used to construct the ARS-A/V5 plasmid were 5′-GAA TTC ATG GCG TTC CTC AAA CTC CG-3′ (forward primer) and 5′-GAA TTC GTA GGT CTC AGA ATC GGA GTC G-3′ (backward primer). The forward PCR primer started at nucleotide 19 to provide an N-terminal methionine for the protein. The insert from the PCR was ligated in-frame with

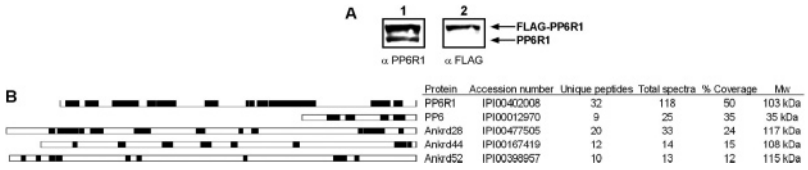

Protein	Accession number	Unique peptides	Total spectra	% Coverage	Mw
PP6R1	IPI00402008	32	118	50	103 kDa
PP6	IPI00012970	9	25	35	35 kDa
Ankrd28	IPI00477505	20	33	24	117 kDa
Ankrd44	IPI00167419	12	14	15	108 kDa
Ankrd52	IPI00398957	10	13	12	115 kDa

FIGURE 1: Proteomics of FLAG-PP6R1-associated proteins by mass spectrometry. (A) Extracts from HEK293 cells stably expressing FLAG-PP6R1 were prepared and analyzed by immunoblotting with anti-PP6R1 (lane 1) and anti-FLAG (lane 2). (B) List of proteins identified in FLAG-PP6R1 immunoprecipitates using mass spectrometry. The schematic on the left is a sequence coverage map depicting as solid bars the location of identified peptides. Shown from left to right are the protein name, the accession number, the number of unique peptide sequences, the number of total peptide spectra, the percent coverage, and the predicted molecular weight for each protein (MW).

the V5 epitope sequence (GKPIPNPLLGLDST) in mammalian expression vector pcDNA3.1/V5-His (Invitrogen, Carlsbad, CA). DNA for human PP6 was amplified by PCR from HeLa cDNA generated by Thermoscript poly(dT) reverse transcription PCR (Invitrogen) following the manufacturer's protocol. PP6 PCR inserts, which matched the open reading frame of NM_002721, were ligated in-frame with HA3 at the BamHI and EcoRI sites in mammalian expression vector pKH3.

Cell Culture and Transfection. HeLa cells were grown in Dulbecco's modified Eagle's medium (GIBCO 11965) containing 10% fetal bovine serum at 37 °C in a humidified 5% CO_2 atmosphere. HEK293 cells were cultured in Eagle's medium (GIBCO 10370) containing 2 mM L-glutamine and 10% fetal bovine serum at 37 °C in a humidified 5% CO_2 atmosphere. HEK293 cells were transiently transfected using Arrest-In (Open Biosystems, Huntsville, AL).

Immunoprecipitation and Immunoblotting. Cells were lysed on culture plates by washing cells with PBS and then adding lysis buffer [50 mM MOPS (pH 7.4), 100 mM NaCl, 0.5% NP-40, 1 mM EGTA, 5% glycerol, Protease Inhibitor Cocktail Set V (concentration as suggested by manufacturer), 1 μM microcystin-LR, and 1 mM dithiothreitol (DTT)]. Cells were incubated in lysis buffer for 20 min on ice, and lysates were centrifuged at 12000*g* (4 °C) for 10 min. Supernatants were used for immunoprecipitation with anti-FLAG beads (M2; Sigma) or anti-V5 beads (Sigma). After rotation with supernatant at 4 °C for 2 h, beads were washed three times in lysis buffer and boiled in 2× SDS sample buffer. SDS−PAGE was carried out according to the method of Laemmli (*25*) using a 29:1 Bio-Rad acrylamide/bisacrylamide mixture (catalog no. 161-0156). The gels were made in three sections: a lower 12% and an upper 8% separating gel to resolve proteins of <50 and >100 kDa, respectively, and a stacking gel. Transfers were done using a TRANS-BLOT SD semidry transfer cell according to the manufacturer's instructions (Bio-Rad, Hercules, CA). Immunoblots were blocked and probed in TBS-T (Tris-buffered saline-Tween 20) buffer containing 3% BSA. Immunoblots were developed using a LI-COR Odyssey Infrared Imaging System scanner (LI-COR Biotechnology), which has a linear response over a 3 log range of intensities.

Subcellular Fractionation and Column Chromatography. Separation of cytoplasm and nuclei was performed using Nuclei EZ Prep kit (NUC101, Sigma) according to the manufacturer's instructions. For chromatography, HeLa cells (5×10^6) were trypsinized from plates, pelleted by centrifugation, washed once, and extracted on ice with 1 mL of 50 mM Tris-HCl (pH 8.0), 1 mM EGTA, 1 mM EDTA, 20 mM β-glycerophosphate, 1% NP-40, and 5 times the recommended amount of protease inhibitor concentrate (Sigma) followed by centrifugation for 20 min at 13600*g*. The supernatant was 5 mg/mL protein, and 0.5 mL was injected onto a diethylaminoethyl (DEAE) MemSep 1000 cartridge (MilliPore Corp.) and eluted at room temperature with a Pharmacia FPLC system at 1.0 mL/min using as buffer A 50 mM Tris-HCl (pH 8.0), 1 mM EDTA, and 75 mM 2-mercaptoethanol and as Buffer B the same composition with 1.0 M NaCl. Elution was carried out for 5 min at 0% B, 20 min from 0 to 35% B, 10 min from 35 to 100% B, and 10 min at 100% B. Fractions were immunoblotted for PP6, PP6R1, and PP6R3. The peak PP6 fractions were pooled and concentrated using a Centricon filter (50 000 molecular weight cutoff), and 0.5 mL was injected onto a Superose 12 (10 mm × 300 mm) column that was eluted at 0.5 mL/min at room temperature in buffer A. The Superose 12 column calibration with nine protein standards and blue dextran is posted at http://www.embl.de/ExternalInfo/protein_unit/draft_frames/protocol_database/Purification/Superose12.pdf.

siRNA Knockdowns. siRNAs were purchased from Dharmacon (Lafayette, CO). siRNAs used as control were designed against luciferase 5′-TAAGGCTATGAAGAGATAC-3′. ARS-A siRNAs tested individually were TCAGAATGCTTACGGCTATTT as the sense sequence for siRNA1, GGAAGGACAGCGTTGCATATT as the sense sequence for siRNA2, and GTAATCGACTGTGAGGATATT as the sense sequence for siRNA3. All three were effective. A Smart pool of siRNA for ARS-A was used for the experiments depicted in Figure 7. PP6R1 siRNA1 was previously described (*21*). PP6R3 siRNAs are GCTCAGAACCGCAAACTTATT as the sense sequence for PP6R3 siRNA1 and CAGAATGTCTCGAAGATTTTT as the sense sequence for PP6R3 siRNA2, and these were combined (60 nM each) for efficient knockdown. Knockdowns were carried out in HeLa cells after cells that had been plated for 24 h were transfected with siRNA (120 nM) using oligofectamine (Invitrogen) following the manufacturer's instructions. After 48 h, fresh medium was added and cells were treated with or without TNFα and lysed in 2× SDS sample buffer.

RESULTS

Proteomics with FLAG-PP6R1 Stably Expressed in 293 Cells. To identify proteins that interact with PP6 holoenzymes, we created a HEK293 cell line stably expressing SAPS domain subunit FLAG-PP6R1. Immunoblotting with anti-PP6R1 showed that the level of the FLAG-tagged protein was only 1.5 times higher than the level of endogenous PP6R1 (Figure 1A). FLAG immunoprecipitates were prepared from 10^7 cells and protein complexes eluted with FLAG peptide and subjected to liquid chromatography−electrospray-Fourier transform ion cyclotron (LC−ESI-

FTICR) mass spectrometry. A total of 84 proteins were identified from peptide sequences, with the greatest number of unique peptides (*32*) from PP6R1 itself (Figure 1B). Proteomics using different FLAG-tagged proteins has shown us that multiple heat shock proteins, cytoskeletal proteins, keratins, and ribosomal proteins are recovered, regardless of the tagged protein used for isolation. We excluded these common contaminants from further analysis. The other binding partners of FLAG-PP6R1 were ranked in terms of coverage of the protein (Figure 1B). The catalytic subunit of PP6 had the fifth best coverage of identified peptides and is an established binding partner for the SAPS domain within PP6R1 (*21*). The other associated proteins were ankyrin repeat proteins of >100 kDa that were individually identified by 10−20 unique peptides, providing 12−24% coverage (Figure 1B). The schematic depicts the positions of the identified peptides in the overall sequences. The total number of spectra and number of unique peptides put these proteins among the top 10 among the 84 proteins identified. These data show the ankyrin repeat proteins stably associate with PP6R1 and raise the possibility that they are PP6 subunits.

Ankyrin Repeat Proteins as Subunits of PP6. The amino acid sequences of Ankrd28, Ankrd44, and Ankrd52, named here ARS-A, ARS-B, and ARS-C, respectively, were aligned for comparison (Figure 2). There is a striking similarity in sequence among these proteins, with greater than 58% overall identity. The first 400 residues comprise a region with nearly identical sequence, compared to the C-terminal region, which shows stretches of variable sequence interspersed among segments of identical sequence. The N- and C-terminal regions are linked by two segments of ∼30 and ∼20 residues that show no identity, within positions 510−600. ARS-A and ARS-C have unique C-terminal tails of >80 residues compared to ARS-B that lacks a tail. A phylogenetic tree of vertebrate homologues of these ankyrin repeat proteins was constructed and rooted to two insect sequences (Figure 2B). This analysis reveals clusters of related proteins for each of three sequences. The conservation of separate sequences reinforces the idea that each of these proteins has a separate biological function. Ankrd28 (ARS-A) appears to be further separated from the two other members of this family. The green pufferfish *Takifugu rubripes* has the smallest known vertebrate genome and has only one related protein composed of ankyrin repeats. This sequence of the presumed ancestral protein aligns most closely with the group exemplified by Ankrd28. We produced antipeptide antibodies for Ankrd28 (ARS-A) to study the endogenous protein.

Subcellular Distribution of Multiple PP6 Subunits. Cell fractionation and immunoblotting demonstrate that PP6 catalytic and regulatory subunits are predominantly cytoplasmic (Figure 3). Adherent HeLa cells and HEK293 cells were dissolved with detergent solution, and the extract was fractionated by centrifugation. The supernatant was collected and designated cytoplasm. The pellet containing nuclei was washed twice by centrifugation and dissolved in SDS sample buffer. Samples of HeLa and HEK293 cytoplasmic and nuclear fractions were immunoblotted for (from top to bottom) PP6R1, ARS-A, PP6-C, and PP6R3, plus the chromatin-associated RanGAP protein RCC1 and cytoplasmic enzyme GAPDH as markers for nuclear and cytoplasmic fractions. PP6 and its SAPS domain subunits PP6R1 and PP6R3 were greater than 95% cytoplasmic, and the endogenous ARS-A subunit exhibited the same distribution, using different antibodies made to the extreme N- and C-terminal sequences of the protein. The appearance of some RCC1 in the cytoplasmic fraction was presumed to be due to release from permeabilized nuclei. The data show a predominant distribution of PP6, PP6R1, and ARS-A together in the cytoplasm of cells.

Coprecipitation of PP6 with Associated Subunits. We expressed V5-tagged ARS-A in HEK293 cells and analyzed coprecipitating proteins. ARS-A was expressed at relatively low levels because it was not detected by anti-V5 immunoblotting of whole cell extracts (Figure 4). The tagged protein was concentrated effectively by anti-V5 immunoprecipitation. The precipitation also concentrated from the extract endogenous PP6 catalytic subunit and endogenous SAPS domain subunits PP6R1 and PP6R3, showing association with ARS-A. PP6 subunit alpha4 was detected in the extracts by direct immunoblotting but did not coprecipitate with V5-tagged ARS-A. Neither PP2A nor PP4 coprecipitated with V5-tagged ARS-A, even though they were detected in the extracts, showing specificity for association of ARS-A with PP6, among closely related phosphatases.

Cells were transfected with HA-PP6, and complexes were recovered by anti-HA immunoprecipitation. HA-PP6 was efficiently precipitated, depleting the cell extract of all detectable HA-tagged protein (Figure 5, top panel). Endogenous PP6R1, PP6R3, and ARS-A were coprecipitated with HA-PP6. However, a substantial fraction of these subunits remained in the supernatant after the immunoprecipitation, probably due to formation of complexes with endogenous PP6. Endogenous PP6R1, PP6R3, and ARS-A proteins did not bind the protein A beads used to recover the antibody, evidenced by a blank control (Figure 5, center lane). Endogenous alpha4 was coprecipitated with HA-PP6 as a positive control for availability and conformational integrity of the ectopic PP6 in cells. Together, the results show the same trio of subunits (PP6, SAPS domain subunit, and ARS-A) were recovered by precipitation of either PP6, SAPS domain subunit, or ARS-A.

Each of the PP6 SAPS domain subunits, PP6R1, PP6R2, and PP6R3, associates with ARS-A. This was demonstrated using four different HEK293 cell lines, each stably expressing either (1) FLAG vector, (2) FLAG-PP6R1, (3) FLAG-PP6R2, or (4) FLAG-PP6R3 (Figure 6A). Immunoprecipitates from these cell lines using anti-FLAG M2 beads were analyzed by immunoblotting. No FLAG-tagged protein was detected in the control extracts, and intensely stained proteins of the correct size were seen for FLAG-PP6R1, FLAG-PP6R2, or FLAG-PP6R3 (Figure 6A, top panel). Each of these SAPS domain subunits coprecipitated endogenous ARS-A and endogenous PP6 catalytic subunit (Figure 6A, center panels). We noted that none of these immunoprecipitates contained PP1 that was stained in the extracts (Figure 6A, bottom panel). The coprecipitation of endogenous ARS-A and endogenous PP6 with FLAG-PP6R1 confirms the proteomic analysis from Figure 1. Furthermore, coprecipitation with FLAG-PP6R2 and FLAG-PP6R3 shows that each of the SAPS domain subunits can associate with ARS-A and PP6.

Mapping Separate Regions in PP6R1 for Binding to PP6 and Ankyrin Repeat Subunits. We tested whether the SAPS domain was required for association with ARS-A by expres-

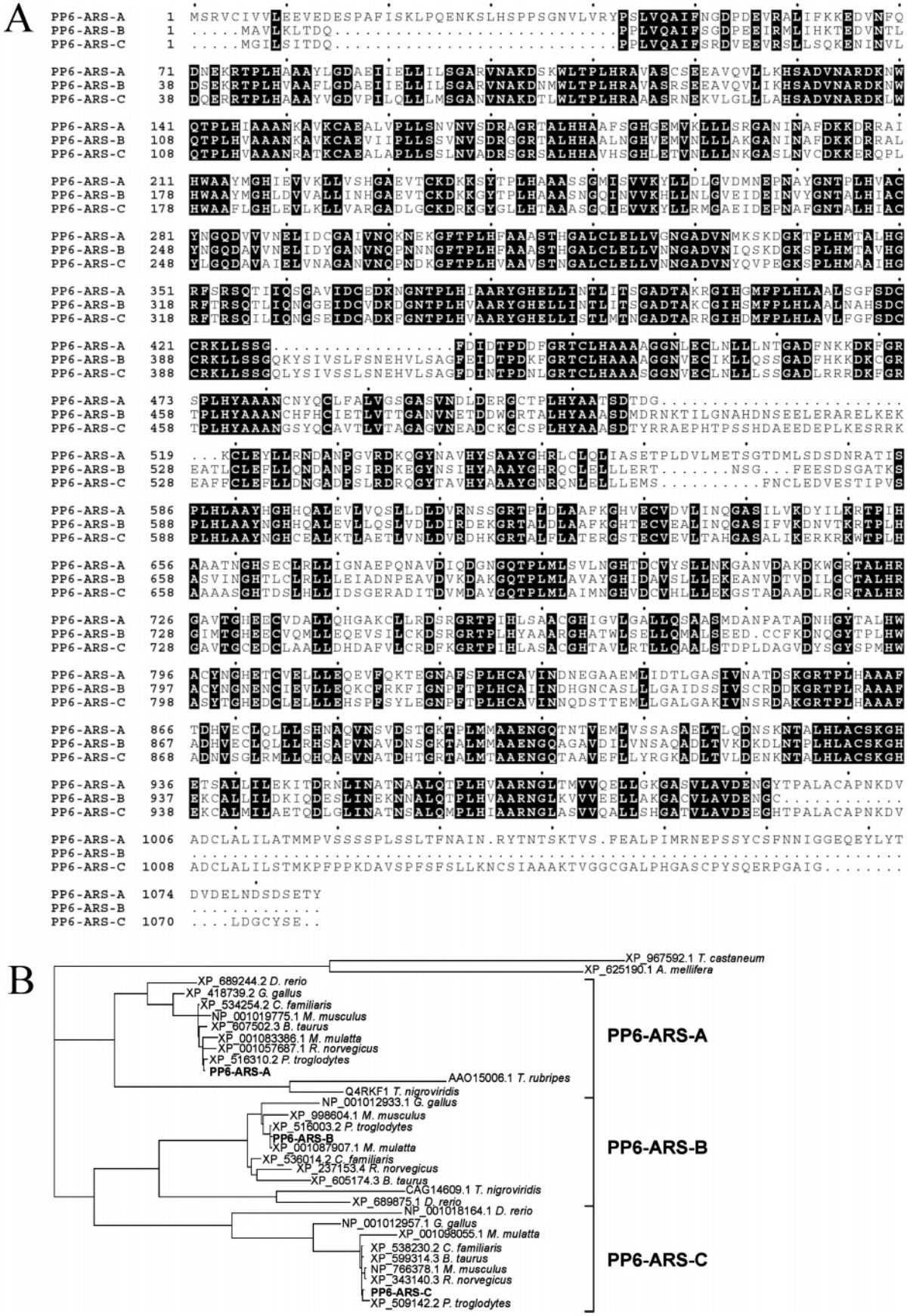

FIGURE 2: Protein sequences of ARS proteins and a phylogenetic tree. (A) Sequences for human ARS-A, ARS-B, and ARS-C were aligned (see Materials and Methods), and identical residues in all three proteins are printed in reverse. (B) A parsimony consensus (rooted) tree was prepared as described in Materials and Methods. Accession numbers of sequences used to construct the phylogenetic tree are included in the figure or Materials and Methods. The tree is divided into three segments labeled ARS-A, ARS-B, and ARS-C.

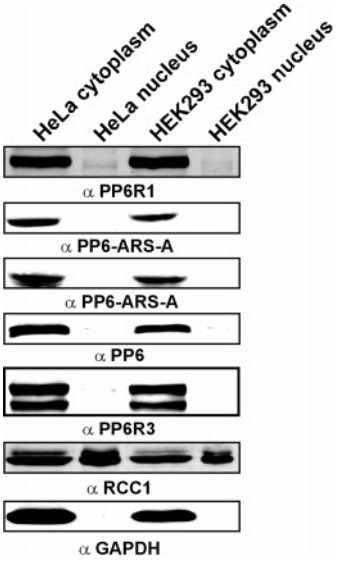

FIGURE 3: Nuclear−cytoplasmic distribution of endogenous PP6 subunits. HeLa and HEK293 cells were lysed and cytoplasmic and nuclear fractions prepared as described in Materials and Methods. Equivalent volumes of fractions were separated by SDS−PAGE on a two-layer (8% top, 12% bottom) gel and immunoblotted with (from top to bottom) anti-PP6R1, anti-ARS-A (N-terminal antibody), anti-ARS-A (C-terminal antibody), anti-PP6, anti-PP6R3, anti-RCC1 (nuclear marker), and anti-GAPDH (cytoplasmic marker) antibodies.

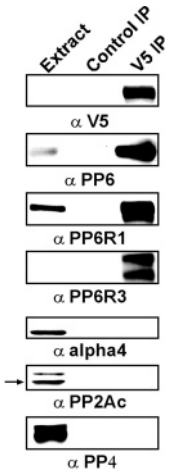

FIGURE 4: Coprecipitation of endogenous PP6, PP6R1, and PP6R3 with V5-tagged ARS-A. ARS-A with a V5 epitope tag was expressed by transient transfection of HEK293 cells. As a negative control, HEK293 cells were mock transfected. Extracts were prepared, and immunoprecipitates were recovered with anti-V5 beads. Immunoprecipitates were resolved by SDS−PAGE as described in the legend of Figure 3 and immunoblotted with (from top to bottom) anti-V5, anti-PP6, anti-PP6R1, anti-PP6R3, anti-alpha4, anti-PP2A, and anti-PP4 antibodies.

sion and immunoprecipitation of full-length FLAG-PP6R1, or truncated FLAG-PP6R1 comprising residues 118−583, 190−583, or 580−943 (Figure 6B). Immunoblotting for FLAG showed recovery of approximately equal amounts of the tagged proteins (Figure 6B, top panel). As demonstrated previously, endogenous PP6 catalytic subunit binds full-length PP6R1 and regions of the protein that encompass the SAPS domain, but not the C-terminal region of the protein outside the SAPS domain (Figure 6B, bottom panel). Interestingly, the converse was true for ARS-A, because it coprecipitated with full-length PP6R1 or with the C-terminal

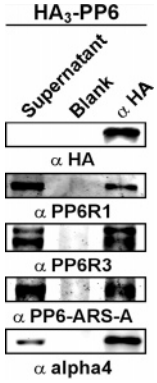

FIGURE 5: Association of HA-tagged PP6 with endogenous SAPS and ankyrin repeat subunits. HEK293 cells were transiently transfected with HA-tagged PP6 catalytic subunit. Extracts were prepared, and protein A agarose was added to lysates without (blank) or with anti-HA antibodies. Precipitated proteins were eluted and resolved by SDS−PAGE as described in the legend of Figure 3 and immunoblotted with (from top to bottom) anti-HA, anti-PP6R1, anti-PP6R3, anti-ARS-A, and anti-alpha4 antibodies.

region (residues 580−943), but not the SAPS domain itself (residues 190−583) or an N-terminal region including the SAPS domain (residues 118−583). The results map interactions to different regions of PP6R1 that are sufficient for formation of stable complexes with different subunits. PP6R1 binds PP6 in its SAPS domain and ARS-A in its C-terminal region.

Chromatography of Endogenous PP6 Holoenzymes. The endogenous PP6 in HeLa cells was partially purified by sequential chromatography to show the presence of trimers composed of the catalytic, SAPS, and ARS subunits. Cell extracts were fractionated by gradient elution from a DEAE matrix, and PP6 eluted as a single major peak from fractions 20−28, with fraction 24 having the largest amount detected by immunoblotting (Figure 7A). This single peak of PP6 encompassed peaks of SAPS domain subunits PP6R3 (fractions 20−24, peak at 22) and PP6R1 (fractions 22−28, peak at 24) that were mostly resolved from one another. Because separate antibodies were used to detect the PP6R1 and PP6R3 subunits, it is not possible to directly compare their relative amounts. However, the distribution of PP6 (compare fraction 22 to 24) indicated that approximately one-third less of the catalytic subunit was associated with PP6R3 compared to PP6R1. Fractions 20−26 from DEAE were pooled, concentrated, and analyzed on a Superose 12 column, where the PP6 eluted as a single major peak (Figure 7B). This peak appears between the elution volume for standards thyroglobulin (8.7 mL, 670 kDa) and ferritin (10.2 mL, 440 kDa). The PP6 catalytic subunit, SAPS domain subunits PP6R1 and PP6R3, and ankyrin repeat subunit ARS-A were all detected in fraction 9 from Superose 12 by immunoblotting, showing copurification in complexes with apparent M_r values of >440 kDa.

Functional Analysis of PP6 Subunits by siRNA Knockdown. Different trimeric PP6 enzymes have separate functions, on the basis of effects of siRNA knockdown of individual subunits. Either PP6R3 or PP6R1 was selectively knocked down by different siRNAs, and ARS-A levels were effectively knocked down by any one of three individual siRNAs (not shown), and by a pool of sequence-specific siRNA. Luciferase siRNA was used as a negative control. Knockdown cells were stimulated with or without TNFα for

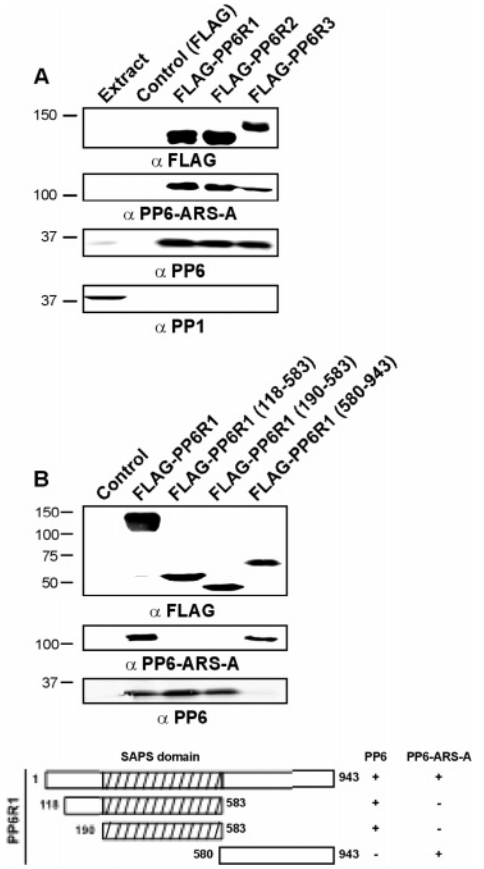

FIGURE 6: Endogenous ARS-A and PP6 associate with stably expressed FLAG-PP6R1, FLAG-PP6R2, and FLAG-PP6R3. (A) Proteins were recovered with anti-FLAG-M2 beads from HEK293 cells stably expressing FLAG-tagged proteins. As a negative control, HEK293 cells with stably integrated FLAG vector alone were used. Proteins in the immunoprecipitates were resolved by SDS−PAGE as described in the legend of Figure 3 and immunoblotted with (from top to bottom) anti-FLAG, anti-ARS-A, anti-PP6, and anti-PP1 antibodies. (B) FLAG-tagged proteins corresponding to residues 118−583, the SAPS domain (residues 190−583), and the C-terminal half (residues 580−943) of PP6R1 were expressed by transient transfection of HEK-293 cells. Immunocomplexes were recovered with anti-FLAG-M2 beads. As positive and negative controls, HEK-293 cells were transfected with either full-length FLAG-PP6R1 or empty plasmid (control). Proteins were resolved by SDS−PAGE as described in the legend of Figure 3 and immunoblotted with anti-FLAG (top panel), anti-ARS-A (center panel), and anti-PP6 (bottom panel) antibodies. The schematic below shows the regions of PP6R1 expressed by the different constructs, and binding of PP6 and ARS-A is indicated by with a plus sign. Migration of molecular weight standards is shown on the left.

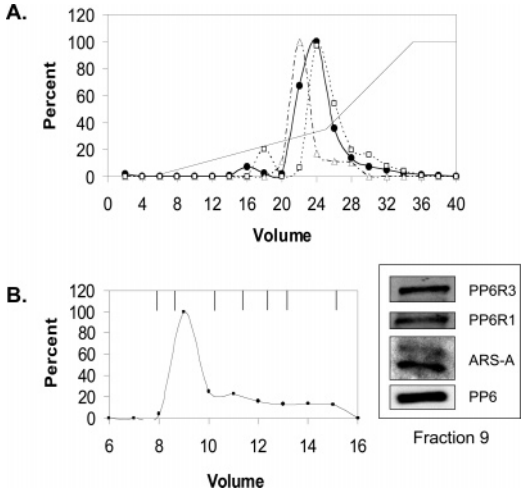

FIGURE 7: Partial purification of PP6 holoenzyme trimers from HeLa cells. The PP6 in HeLa cells was partially purified by sequential chromatography using gradient elution from DEAE (A) and gel permeation on Superose 12 (B) as described in Materials and Methods. (A) Elution of the PP6 catalytic (●), PP6R1 (□), and PP6R3 (△) subunits was monitored by immunoblotting, and the relative amounts were plotted. Fractions 20−26 from DEAE were pooled, concentrated, and resolved on a Superose 12 column. (B) Immunoblotting for PP6 catalytic subunit (●) revealed one peak, and this fraction also contained SAPS subunits (PP6R1 and PP6R3) and ankyrin repeat subunit ARS-A. The bars in the top of the frame indicate the published elution volumes from Superose 12 (10 × 300) for (from left to right) blue dextran (V_0), thyroglobulin (670 kDa), ferritin (440 kDa), catalase (232 kDa), γ-globulin (158 kDa), albumin (67 kDa), and ovalbumin (44 kDa). Fraction 9 from Superose 12 was concentrated 4-fold by SpeedVac evaporation, and 25 μL was immunoblotted for PP6R3, PP6R1, ARS-A, and PP6, using individual antibodies.

30 min to activate the NF-κB pathway, and we measured the fraction of IκBϵ remaining in knockdown cells. Cells knocked down for ARS-A showed a statistically significant reduction in the fraction of IκBϵ remaining after TNFα (Figure 8). This level of residual IκBϵ was about 2-fold lower than in cells knocked down for luciferase and treated with TNFα. Knockdown of PP6R1 showed an identical significant reduction in the fraction of IκBϵ remaining as cells knocked down for ARS-A. Because knockdown of PP6R1 reduced the level of IκBϵ to the exact same level as knockdown of ARS-A, these two proteins are functionally equivalent in this assay. On the other hand, TNFα-induced degradation of IκBϵ was the same in cells knocked down for PP6R3 or for luciferase. These results support the proposal that PP6R1 and ARS-A are subunits of the same specific PP6 holoenzyme.

DISCUSSION

This study presents new evidence that PP6 is a heterotrimeric enzyme composed of a catalytic domain, a SAPS domain subunit, and an ankyrin repeat subunit (ARS). Stably overexpressed SAPS domain subunit PP6R1 associated with PP6 catalytic subunit plus a family of three endogenous cellular proteins that were identified by mass spectrometry. These ankyrin repeat proteins we named ARS-A, ARS-B, and ARS-C. Epitope-tagged catalytic, SAPS, or ARS subunits reciprocally co-immunoprecipitated the other two endogenous subunits. The ARS subunit associated with the C-terminal region of PP6R1 without the SAPS domain, whereas the SAPS domain associates with PP6 catalytic subunit. Partial purification of PP6 from HeLa cells by sequential chromatography yielded complexes with apparent M_r values of >440 kDa. Knockdown of PP6R1, but not PP6R3, produced the same effects as knockdown of ARS-A, suggesting individual heterotrimers with specific functions. Presumably, sequences in the C-terminal region of the different SAPS subunits determine specificity for binding to ARS. This subunit arrangement for PP6 is reminiscent of the ABC heterotrimer of PP2A phosphatase. The A subunit is composed of helical HEAT repeats in a horseshoe-shaped scaffold, and the opposite ends of the subunit bind the catalytic (C) and regulatory (B) subunits side by side on one face of the scaffold (*27*, *28*). We propose the SAPS domain

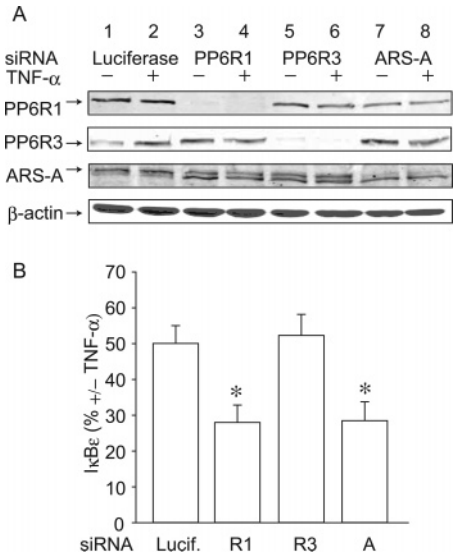

FIGURE 8: Enhanced IκBϵ degradation by siRNA knockdown of ARS-A or PP6R1. (A) HeLa cells in 12-well plates were treated for 48 h with siRNA against luciferase as a control (lanes 1 and 2), an individual siRNA for PP6R1 (lanes 3 and 4), a mixture of two siRNAs for PP6R3 (lanes 5 and 6), and a SmartPool of siRNA for ARS-A (lanes 7 and 8). Parallel samples were untreated (odd-numbered lanes) or treated with 20 ng/mL TNFa for 30 min (even-numbered lanes). Cells were extracted and immunoblotted for PP6R1, PP6R3, ARS-A, and IκBϵ, with β-actin as a loading control. (B) HeLa cell extracts were analyzed by immunoblotting for the fractional amount of IκBϵ remaining after TNFα stimulation (compared to the IκBϵ in cells without added TNFα, set as 1.0). Protein levels were quantitated on the basis of fluorescence intensity determined with an Odyssey Infrared Scanner (Li-Cor Industries) and normalized for loading to actin. The results are from three independent experiments, and the means $\pm$ the standard deviation were analyzed by Student's t test ($p < 0.001$).

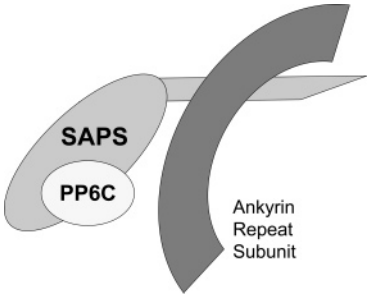

FIGURE 9: Model for PP6 holoenzyme trimers. The model depicts the PP6 catalytic subunit as a spheroid, based on other PPP structures, bound to the SAPS domain region of the subunit that acts as a scaffold, with a C-terminus that alone is sufficient for association with an ankyrin repeat subunit. Ankyrin has an extended arc-like structure composed of helix repeats.

subunit serves primarily as a scaffold, to bind PP6 catalytic and ankyrin repeat subunits into a trimer.

The sequences of these ARSs for PP6 are extensively identical to one another, but they form three branches on a phylogenetic tree for vertebrate species. This argues that each ARS serves separate biological functions that have been preserved during evolution. We propose that the biological functions of PP6 are determined by different heterotrimers, formed by a specific combination of SAPS and ARS subunits. Ankyrin repeats are structures formed by α-helices that appear in tandem and are utilized for protein−protein interactions (*29*). Prominent examples with known three-dimensional structures are IκB, MYPT1, Notch, p16^{INK}, and p53BP2 (*29*). The ankyrin repeat proteins have relatively extended structures. This probably contributes to the apparent M_r of PP6 holoenzymes by gel filtration being larger than the sum of the subunit masses. We expect that the ARS subunits will fulfill a role similar to that of the B subunits of PP2A and be involved in the recognition of phosphoprotein substrates.

In *S. cerevisiae*, the protein Ser/Thr phosphatase Sit4, the homologue of PP6, forms separate dimers with three different SAP (Sit4-associated proteins) subunits: SAP155, SAP185, and SAP190 (*2*, *20*). The evidence was based on co-immunoprecipitation from metabolically labeled cells, and had there been additional subunits, they would likely have been detected. This established that the Sit4 phosphatase used regulatory subunits that were distinct from the subunits for Pph21/22, the yeast PP2A. We found human homologues of the SAP proteins and demonstrated that they selectively associated with PP6 but not closely related phosphatase catalytic subunits PP2A and PP4 (*21*). Therefore, it was reasonable to initially conclude that human PP6 formed heterodimers with SAPS domain subunits, like the Sit4 and SAP proteins in yeast. However, we identified ankyrin repeat proteins in a complex with PP6 and SAPS domain subunits. This complex of proteins had been recovered independently by TAP tagging of IκBϵ, implicating PP6 in regulation of NFκB signaling (*30*). We have used the ankyrin repeat sequences to search the yeast genome by BLAST but did not identify a candidate homologue. Perhaps this is not surprising because yeast do not have a NFκB signaling system.

Physical association and functional specificity support the proposal that these ankyrin repeat proteins act as PP6 subunits. Subcellular fractionation and immunoblotting demonstrated that endogenous ARS-A was predominantly cytoplasmic, as were most of the endogenous PP6, and PP6R1 and PP6R3 subunits, localizing the different subunits in the same subcellular compartment. Phosphopeptides from PP6R3 have been identified in HeLa nuclear extracts (*31*), and PP6 catalytic subunit has been observed in nuclear extracts (*32*); therefore, at least some fraction of PP6 is in the nucleus. Certain PP6 holoenzymes may undergo nucleo-cytoplasmic shuttling. Overexpression of V5-tagged ARS-A or FLAG-tagged PP6R1, PP6R2, or PP6R3 showed association with endogenous partners by co-immunoprecipitation. However, in these experiments, a single ARS associated with multiple SAPS subunits and a single SAPS subunit associated with multiple ARS. One interpretation of these data is that the SAPS and ARS subunits can associate pairwise in a variety of combinations. Nonspecific combinations would produce nine (3×3) different holoenzymes from three SAPS subunits and three ARS subunits. On the other hand, siRNA knockdown showed that PP6R1 and ARS-A were functionally equivalent, and distinct from PP6R3. On the basis of these results, we favor a model in which there are three primary PP6 holoenzymes, each with a unique pair of SAPS and ARS subunits (e.g., PP6R1::ARS-A).

The ankyrin repeat proteins identified here are expected to have important roles in determining the specificity and regulation of PP6 phosphatase. Consistent with assignment as a phosphatase subunit, ARS-A (Ankrd28, KIAA0379) was identified in a proteomic analysis of proteins bound to immobilized microcystin (*23*). Microcystin is an active site

inhibitor of the PPP phosphatase family and can be used to isolate holoenzyme complexes of PP1, PP2A, PP4, and PP6. Among the proteins bound to microcystin, PP6R1 (KIAA1115) and PP6R3 (SAPLB) also were identified by mass spectrometry, suggesting that PP6 holoenzyme complexes were recovered (*23*). Ankyrin repeat protein KIAA0379 coprecipitated with PP1 catalytic subunit and therefore was called PITK (phosphatase interactor targeting K protein). These investigators went on to show phosphorylation of PITK and coprecipitation with hnRNP K, suggesting that PITK serves as a regulatory and substrate targeting subunit for PP1. We detected endogenous PP1 in immunoprecipitates of tagged KIAA0379, confirming that the two proteins can associate together. However, we did not find PP1 associated with the SAPS subunits for PP6, by either immunoblotting or mass spectrometry, whereas ankyrin repeat protein KIAA0379 (ARS-A) was identified readily in the SAPS subunit complexes by both immunoblotting and mass spectrometry. Our interpretation of these results is that KIAA0379 can associate with PP1 but does not associate with PP1 and SAPS domain subunits at the same time in the same complex. Perhaps KIAA0379 has alternate functions, as either PITK or ARS-A, and forms separate complexes with PP1 or PP6. KIAA0379 appears in gene array analysis to be upregulated in response to infection with *Ehrlichia chaffeensis* (*33*), or treatment with CpG-ODN (*34*), or in CML cells (*35*). KIAA0379 is reported to be phosphorylated by CaMKII and GSK3 (*36*), and we have evidence that PP6R1 also has multiple phosphorylation sites (unpublished), raising the possibility that phosphorylation of regulatory subunits regulates PP6, through either enzyme activity, subunit assembly, intracellular localization, or substrate specificity. Regulation and function of individual PP6 heterotrimers remain to be elucidated.

ACKNOWLEDGMENT

We thank Michael B. Black (University of Virginia, Academic Computing Health Sciences) for generating the phylogenetic tree. We thank Timothy Haystead and Nicole Kwiek for constructs and antibodies to PITK and Todd D. Prickett for preparation of HA_3-PP6.

REFERENCES

1. Fernandez-Sarabia, M. J., Sutton, A., Zhong, T., and Arndt, K. T. (1992) SIT4 protein phosphatase is required for the normal accumulation of SWI4, CLN1, CLN2, and HCS26 RNAs during late G1, *Genes Dev. 6*, 2417−2428.
2. Sutton, A., Immanuel, D., and Arndt, K. T. (1991) The SIT4 protein phosphatase functions in late G_1 for progression into S phase, *Mol. Cell. Biol. 11*, 2133−2148.
3. Clotet, J., Gari, E., Aldea, M., and Arino, J. (1999) The yeast ser/thr phosphatases sit4 and ppz1 play opposite roles in regulation of the cell cycle, *Mol. Cell. Biol. 19*, 2408−2415.
4. Hayashi, N., Nomura, T., Sakumoto, N., Mukai, Y., Kaneko, Y., Harashima, S., and Murakami, S. (2005) The SIT4 gene, which encodes protein phosphatase 2A, is required for telomere function in *Saccharomyces cerevisiae*, *Curr. Genet. 47*, 359−367.
5. Manlandro, C. M., Haydon, D. H., and Rosenwald, A. G. (2005) Ability of Sit4p to promote K^+ efflux via Nha1p is modulated by Sap155p and Sap185p, *Eukaryotic Cell 4*, 1041−1049.
6. Shirra, M. K., Rogers, S. E., Alexander, D. E., and Arndt, K. M. (2005) The Snf1 protein kinase and Sit4 protein phosphatase have opposing functions in regulating TATA-binding protein association with the *Saccharomyces cerevisiae* INO1 promoter, *Genetics 169*, 1957−1972.
7. Rohde, J. R., Campbell, S., Zurita-Martinez, S. A., Cutler, N. S., Ashe, M., and Cardenas, M. E. (2004) TOR controls transcriptional and translational programs via Sap-Sit4 protein phosphatase signaling effectors, *Mol. Cell. Biol. 24*, 8332−8341.
8. Singer, T., Haefner, S., Hoffmann, M., Fischer, M., Ilyina, J., and Hilt, W. (2003) Sit4 phosphatase is functionally linked to the ubiquitin-proteasome system, *Genetics 164*, 1305−1321.
9. Wang, H., Wang, X., and Jiang, Y. (2003) Interaction with Tap42 is required for the essential function of Sit4 and type 2A phosphatases, *Mol. Biol. Cell 14*, 4342−4351.
10. Angeles de la Torre-Ruiz, M., Torres, J., Arino, J., and Herrero, E. (2002) Sit4 is required for proper modulation of the biological functions mediated by Pkc1 and the cell integrity pathway in *Saccharomyces cerevisiae*, *J. Biol. Chem. 277*, 33468−33476.
11. Jablonowski, D., Butler, A. R., Fichtner, L., Gardiner, D., Schaffrath, R., and Stark, M. J. (2001) Sit4p protein phosphatase is required for sensitivity of *Saccharomyces cerevisiae* to *Kluyveromyces lactis* zymocin, *Genetics 159*, 1479−1489.
12. Masuda, C. A., Ramirez, J., Pena, A., and Montero-Lomeli, M. (2000) Regulation of monovalent ion homeostasis and pH by the Ser-Thr protein phosphatase SIT4 in *Saccharomyces cerevisiae*, *J. Biol. Chem. 275*, 30957−30961.
13. Posas, F., Clotet, J., and Arino, J. (1991) *Saccharomyces cerevisiae* gene SIT4 is involved in the control of glycogen metabolism, *FEBS Lett. 279*, 341−345.
14. Jablonka, W., Guzman, S., Ramirez, J., and Montero-Lomeli, M. (2006) Deviation of carbohydrate metabolism by the SIT4 phosphatase in *Saccharomyces cerevisiae*, *Biochim. Biophys. Acta 1760*, 1281−1291.
15. Tate, J. J., Feller, A., Dubois, E., and Cooper, T. G. (2006) *Saccharomyces cerevisiae* Sit4 phosphatase is active irrespective of the nitrogen source provided, and Gln3 phosphorylation levels become nitrogen source-responsive in a sit4-deleted strain, *J. Biol. Chem. 281*, 37980−37992.
16. Stark, M. J. (1996) Yeast protein serine/threonine phosphatases: Multiple roles and diverse regulation, *Yeast 12*, 1647−1675.
17. Zabrocki, P., Van Hoof, C., Goris, J., Thevelein, J. M., Winderickx, J., and Wera, S. (2002) Protein phosphatase 2A on track for nutrient-induced signalling in yeast, *Mol. Microbiol. 43*, 835−842.
18. Mann, D. J., Dombradi, V., and Cohen, P. T. (1993) *Drosophila* protein phosphatase V functionally complements a SIT4 mutant in *Saccharomyces cerevisiae* and its amino-terminal region can confer this complementation to a heterologous phosphatase catalytic domain, *EMBO J. 12*, 4833−4842.
19. Bastians, H., and Ponstingl, H. (1996) The novel human protein serine/threonine phosphatase 6 is a functional homologue of budding yeast Sit4p and fission yeast ppe1, which are involved in cell cycle regulation, *J. Cell Sci. 109*, 2865−2874.
20. Luke, M. M., Della Seta, F., Di Como, C. J., Sugimoto, H., Kobayashi, R., and Arndt, K. T. (1996) The SAP, a new family of proteins, associate and function positively with the SIT4 phosphatase, *Mol. Cell. Biol. 16*, 2744−2755.
21. Stefansson, B., and Brautigan, D. L. (2006) Protein phosphatase 6 subunit with conserved Sit4-associated protein domain targets IκBε, *J. Biol. Chem. 281*, 22624−22634.
22. Murata, K., Wu, J., and Brautigan, D. L. (1997) B cell receptor-associated protein alpha4 displays rapamycin-sensitive binding directly to the catalytic subunit of protein phosphatase 2A, *Proc. Natl. Acad. Sci. U.S.A. 94*, 10624−10629.
23. Kwiek, N. C., Thacker, D. F., Datto, M. B., Megosh, H. B., and Haystead, T. A. (2006) PITK, a PP1 targeting subunit that modulates the phosphorylation of the transcriptional regulator hnRNP K, *Cell Signalling 18*, 1769−1778.
24. Gouet, P., Courcelle, E., Stuart, D. I., and Metoz, F. (1999) ESPript: Analysis of multiple sequence alignments in PostScript, *Bioinformatics 15*, 305−308.
25. Laemmli, U. K. (1970) Cleavage of structural proteins during the assembly of the head of bacteriophage T4, *Nature 227*, 680−685.
26. Prickett, T. D., and Brautigan, D. L. (2007) Cytokine activation of p38 MAPK and apoptosis is opposed by alpha-4 targeting of PP2A for site-specific dephosphorylation of MEK3, *Mol. Cell. Biol. 27*, 4217−4227.
27. Cho, U. S., and Xu, W. (2007) Crystal structure of a protein phosphatase 2A heterotrimeric holoenzyme, *Nature 445*, 53−57.
28. Xu, Y., Xing, Y., Chen, Y., Chao, Y., Lin, Z., Fan, E., Yu, J. W., Strack, S., Jeffrey, P. D., and Shi, Y. (2006) Structure of the protein phosphatase 2A holoenzyme, *Cell 127*, 1239−1251.

29. Mosavi, L. K., Cammett, T. J., Desrosiers, D. C., and Peng, Z. Y. (2004) The ankyrin repeat as molecular architecture for protein recognition, *Protein Sci. 13*, 1435−1448.
30. Bouwmeester, T., Bauch, A., Ruffner, H., Angrand, P. O., Bergamini, G., Croughton, K., Cruciat, C., Eberhard, D., Gagneur, J., Ghidelli, S., Hopf, C., Huhse, B., Mangano, R., Michon, A. M., Schirle, M., Schlegl, J., Schwab, M., Stein, M. A., Bauer, A., Casari, G., Drewes, G., Gavin, A. C., Jackson, D. B., Joberty, G., Neubauer, G., Rick, J., Kuster, B., and Superti-Furga, G. (2004) A physical and functional map of the human TNF-α/NF-κB signal transduction pathway, *Nat. Cell Biol. 6*, 97−105.
31. Beausoleil, S. A., Jedrychowski, M., Schwartz, D., Elias, J. E., Villen, J., Li, J., Cohn, M. A., Cantley, L. C., and Gygi, S. P. (2004) Large-scale characterization of HeLa cell nuclear phosphoproteins, *Proc. Natl. Acad. Sci. U.S.A. 101*, 12130−12135.
32. Shi, Y., Reddy, B., and Manley, J. L. (2006) PP1/PP2A phosphatases are required for the second step of Pre-mRNA splicing and target specific snRNP protein, *Mol. Cell 23*, 819−829.
33. Zhang, J. Z., Sinha, M., Luxon, B. A., and Yu, X. J. (2004) Survival strategy of obligately intracellular *Ehrlichia chaffeensis*: Novel modulation of immune response and host cell cycles, *Infect. Immun. 72*, 498−507.
34. Kuo, C. C., Kuo, C. W., Liang, C. M., and Liang, S. M. (2005) A transcriptomic and proteomic analysis of the effect of CpG-ODN on human THP-1 monocytic leukemia cells, *Proteomics 5*, 894−906.
35. Kaneta, Y., Kagami, Y., Tsunoda, T., Ohno, R., Nakamura, Y., and Katagiri, T. (2003) Genome-wide analysis of gene-expression profiles in chronic myeloid leukemia cells using a cDNA microarray, *Int. J. Oncol. 23*, 681−691.
36. Kwiek, N. C., Thacker, D. F., and Haystead, T. A. (2007) Dual kinase-mediated regulation of PITK by CaMKII and GSK3, *Cell. Signalling 19*, 593−599.

BI7022877